

Sinoatrial Nodal Cell Ryanodine Receptor and Na⁺-Ca²⁺ Exchanger Molecular Partners in Pacemaker Regulation

Konstantin Y. Bogdanov, Tatiana M. Vinogradova, Edward G. Lakatta

Abstract—The rate of spontaneous diastolic depolarization (DD) of sinoatrial nodal cells (SANCs) that triggers recurrent action potentials (APs) is a fundamental aspect of the heart's pacemaker. Here, in experiments on isolated SANCs, using confocal microscopy combined with a patch clamp technique, we show that ryanodine receptor Ca²⁺ release during the DD produces a localized subsarcolemmal Ca²⁺ increase that spreads in a wavelike manner by Ca²⁺-induced Ca²⁺ release and produces an inward current via the Na⁺-Ca²⁺ exchanger (NCX). Ryanodine, a blocker of the sarcoplasmic reticulum Ca²⁺ release channel, in a dose-dependent manner reduces the SANC beating rate with an IC₅₀ of 2.6 μmol/L and abolishes the local Ca²⁺ transients that precede the AP upstroke. In voltage-clamped cells in which the DD was simulated by voltage ramp, 3 μmol/L ryanodine decreased an inward current during the voltage ramp by 1.6±0.3 pA/pF (SEM, n=4) leaving the peak of L-type Ca²⁺ current unchanged. Likewise, acute blockade of the NCX (via rapid substitution of bath Na⁺ by Li⁺) abolished SANC beating and reduced the inward current to a similar extent (1.7±0.4 pA/pF, n=4), as did ryanodine. Thus, in addition to activation/inactivation of multiple ion channels, Ca²⁺ activation of the NCX, because of localized sarcoplasmic reticulum Ca²⁺ release, is a critical element in a chain of molecular interactions that permits the heartbeat to occur and determines its beating rate. (*Circ Res.* 2001;88:1254-1258.)

Key Words: sinoatrial node ■ automaticity ■ ryanodine receptor ■ Na⁺-Ca²⁺ exchange

Although it is generally assumed that multiple ionic channel currents including L-type (I_{CaL}) and T-type (I_{CaT}) Ca²⁺ currents, the hyperpolarization-activated current (I_i), slow and rapid delayed rectifying K⁺ currents, sustained and background,^{1,2} transient outward current, and Na⁺-K⁺ pump and Na⁺-Ca²⁺ exchanger currents³ underlie the sinoatrial nodal cell (SANC) diastolic depolarization (DD) and regulate its slope and thus the spontaneous beating rate,⁴⁻⁶ the specific role of each of these in determining the rate of action potential (AP) firing remains to be established. As in ventricular myocytes, the SANC AP is accompanied by a transient increase in cytosolic Ca²⁺ concentration ($[Ca^{2+}]_i$),⁷⁻¹⁰ which in myocytes occurs via release from the sarcoplasmic reticulum (SR) via ryanodine-sensitive Ca²⁺-induced Ca²⁺ release (CICR).¹¹ In ventricular myocytes, the AP initiates synchronized Ca²⁺ release via *t*-tubular depolarization-induced activation of I_{CaL} and CICR to produce a contraction that results from the ensuing Ca²⁺ myofilament interaction. SANCs, in contrast, contain little contractile material, which is rather haphazardly distributed within them, and have no *t*-tubular system to synchronize Ca²⁺ release from SR throughout the cell.¹² Thus, it has not been intuitively clear why the SANC AP should be associated with a $[Ca^{2+}]_i$

transient. However, a recent study in spontaneously beating cat atrial pacemaker cells¹⁰ has detected an increase in subsarcolemmal $[Ca^{2+}]_i$ that occurs before the AP upstroke. This and other observations³ have provided indirect evidence to suggest that Ca²⁺-dependent modulation of the SANC DD slope via the Na⁺-Ca²⁺ exchanger (NCX), an interaction that generates inward current, is involved in spontaneous SANC beating and thus in SANC pacemaker function. However, the characteristics of this localized pre-AP release in isolated SANCs have not been determined. In addition, the extent to which the forward mode of electrogenic NCX activated by Ca²⁺ release from SR contributes to the DD and modulates the SANC beating rate is unknown.

Therefore, the present study specifically characterized localized pre-AP Ca²⁺ release in isolated rabbit SANCs, characterized the current generated by its activation of the NCX, and determined the effect of this coordinated operation of ryanodine receptors (RYRs) and NCX on spontaneous SANC beating rate. Our findings indicate that in SANC pre-AP Ca²⁺ releases are locally propagating Ca²⁺ waves resulting from ryanodine-sensitive CICR. A negative chronotropic effect of ryanodine is accompanied by disappearance of the localized pre-AP Ca²⁺ releases. The present results also

Original received February 9, 2001; revision received April 26, 2001; accepted April 26, 2001.

From the Laboratory of Cardiovascular Science, Gerontology Research Center, National Institute on Aging, National Institutes of Health, Baltimore, Md.

Correspondence to Konstantin Bogdanov, PhD, Laboratory of Cardiovascular Sciences, Gerontology Research Center, NIA, NIH, 5600 Nathan Shock Dr, Baltimore, MD 21224. E-mail BogdanovK@grc.nia.nih.gov

© 2001 American Heart Association, Inc.

Circulation Research is available at <http://www.circresaha.org>

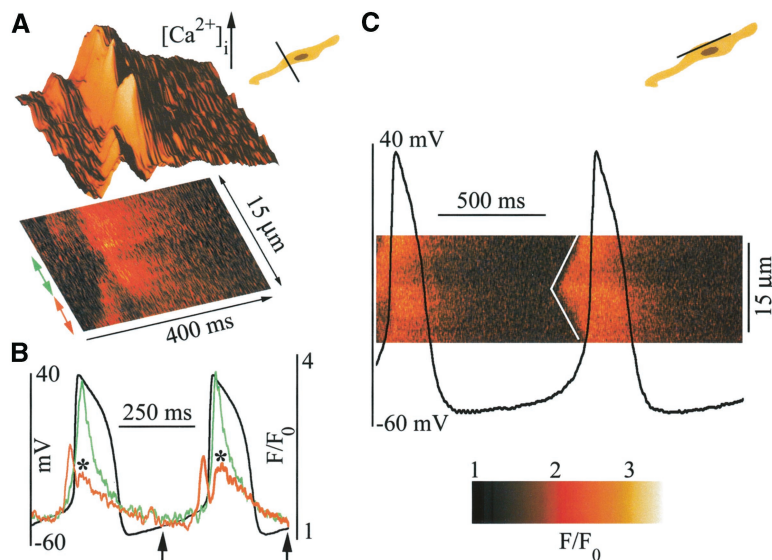


Figure 1. Spatial distribution of Ca^{2+} release in rabbit SANCs. A, Linescan image of Ca^{2+} release (bottom) and corresponding normalized fluorescence (top) depicted as a function of time and position within the scanline that is perpendicular to the cell long axis (inset). Two-color, double-headed arrows show areas where fluorescence was averaged. B, Membrane potential (black) and normalized fluorescence averaged spatially near the edge (red) and middle (green) of the cell. Two single-headed arrows demarcate a time interval during which 3-dimensional distribution was plotted. *Second peak in the Ca^{2+} release near the cell edge. Note that initial $[\text{Ca}^{2+}]_i$ elevation occurs locally near the cell edge before AP upstroke. C, Wavelike pattern of $[\text{Ca}^{2+}]_i$ spread in SANCs. Linescan image of Ca^{2+} release and membrane potential recording in SANCs with the scanline oriented parallel to long cell axis near cell edge. Two white lines were drawn to facilitate visualization of Ca^{2+} propagation from a point located near the intersection of the lines.

provide an estimate of the density of NCX current generated during the DD and demonstrate that acute blockade of NCX stops the spontaneous SANC beating. Taken together these results provide direct evidence of the mechanism by which the localized pre-AP Ca^{2+} releases from SR accelerate SANC beating rate via activation of forward mode electrogenic NCX.

Materials and Methods

Single rabbit SANCs were isolated as described previously,¹³ using protocols approved by our institution's Animal Care and Use Committee, and then loaded with fluo-3-acetoxymethyl ether (Molecular Probes). Cells chosen for the study had a spindle-like or spider-like shape. A LSM-410 microscope (Carl Zeiss, Inc) was used to image the cells. IDL software (version 5.2, Research System Inc) was used for data analysis. The fluo-3 fluorescence signal (F) was normalized by the minimal value between beats (F_0). Images were acquired in the confocal linescan mode, which repeatedly scans a single line through the cell every 1.39 to 5 ms. The lines are plotted vertically, and each line is added to the right of the preceding line to form the linescan image. In these images, time increases from left to right and vertical displacement corresponds to position along the scanline. Perforated or ruptured patch clamps using Axopatch-200B amplifier (Axon Instruments) were used to record spontaneous APs or membrane currents, respectively. Pipettes were filled with (in mmol/L) potassium gluconate 120, KCl 20, NaCl 5, HEPES 5, and MgATP 5 (pH 7.2). The extracellular bathing solution contained (in mmol/L) NaCl 140, KCl 5.4, MgCl_2 1, HEPES 5, CaCl_2 1.8, and glucose 5.5 (pH 7.4). For perforated-patch experiments, β -escin (50 $\mu\text{mol/L}$) was added to pipette solution. For membrane current recordings, 10 $\mu\text{mol/L}$ tetrodotoxin was added to block the fast Na^+ current. All experiments were performed at 34°C. Data are expressed as mean \pm SEM. Significance was determined using the Student t test (significance level, $P < 0.05$).

Results and Discussion

Figure 1A shows a 3-dimensional reconstruction of a linescan image of $[\text{Ca}^{2+}]_i$ with the scanned line perpendicular to the longitudinal axis of the cell, crossing it at half of its depth (inset in upper right). It is known that SANCs lack t -tubules, and therefore a spreading of a local Ca^{2+} release via the CICR mechanism from the cell surface to more centered corbular SR sometimes takes several tens of milliseconds.^{14,15} This accounts for the U-shaped pattern illustrated by the

3-dimensional image of the $[\text{Ca}^{2+}]_i$ in Figure 1A. Thus, Ca^{2+} waves propagating from the surface toward the center (see Figure 1A) can amplify the small initial subsarcolemmal release, which explains the mechanism by which $[\text{Ca}^{2+}]_i$ rises to a high value in the middle of the cell. If the scanned line oriented perpendicular to the long cell axis is moved from the cell depth toward sarcolemma or is not perfectly perpendicular, the U-shaped pattern of linescan image is not visible so clearly (compare Figure 3B versus Figure 1A).

Figure 1B shows the $[\text{Ca}^{2+}]_i$ and membrane potential recordings before and during a spontaneous beat. Note that in panel B, at the cell edges, a local $[\text{Ca}^{2+}]_i$ transient precedes the AP upstroke. In 68 measured beats, the subsarcolemmal $[\text{Ca}^{2+}]_i$ occurred 106 ± 7 ms before the global $[\text{Ca}^{2+}]_i$ transient. The pre-AP $[\text{Ca}^{2+}]_i$ increases were localized within small regions beneath sarcolemma and thus could be recorded only when a scanned line passed through these regions. (Because only a single line was scanned in each cell, the pre-AP $[\text{Ca}^{2+}]_i$ transients could not be recorded in 14 of 53 cells.) In 39 cells, detectable $[\text{Ca}^{2+}]_i$ transients localized to the cell edge occurred 70 ± 5 ms before the AP upstroke (see red curve in Figure 1B). Note that, in contrast, the $[\text{Ca}^{2+}]_i$ transient detected across the middle part of the cell width (green curve in Figure 1B) peaks after the AP peak, ie, as it does in ventricular myocytes. In some cells, the pre-AP $[\text{Ca}^{2+}]_i$ transient had characteristics similar to that of Ca^{2+} sparks¹⁶; in other cases (eg, see Figure 1A), the pre-AP $[\text{Ca}^{2+}]_i$ transient propagated from the cell edge to its interior as a Ca^{2+} wave. The spatial dimension histogram of pre-AP $[\text{Ca}^{2+}]_i$ transients demonstrated a peak between 3 and 4 μm ; the average spatial size was 5.9 ± 0.4 μm ($n = 96$). The duration of the pre-AP $[\text{Ca}^{2+}]_i$ transient at half amplitude was 56 ± 3 ms ($n = 73$). Most pre-AP $[\text{Ca}^{2+}]_i$ transients exhibited spatial heterogeneity having a multifocal pattern of release.

When the scanned line is positioned parallel to the longitudinal axis of the cell and close to the sarcolemmal membrane (Figure 1C), the local subsarcolemmal $[\text{Ca}^{2+}]_i$ transient exhibits an early component that precedes the AP upstroke, and the spatial pattern of the early $[\text{Ca}^{2+}]_i$ transient exhibits

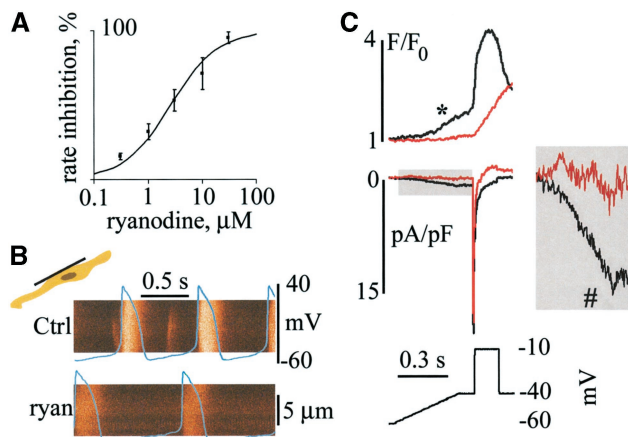


Figure 2. Ryanodine inhibits SANC beating rate (A), pre-AP spontaneous $[Ca^{2+}]_i$ increase (B), and inward current and $[Ca^{2+}]_i$ increase during DD without affecting peak $I_{Ca,L}$ (C). A, Dose dependence of the ryanodine inhibitory effect on the spontaneous AP firing rate. B, Linescan image of Ca^{2+} release with superimposed AP records (blue) in control (Ctrl) and 1 minute after addition of 3 $\mu\text{mol/L}$ ryanodine (ryan). Scanline is oriented parallel to long cell axis near cell edge (inset). C, Normalized fluorescence (top) and membrane current (left middle) under voltage clamp before (black) and 4 minutes after (red) addition of 3 $\mu\text{mol/L}$ ryanodine; voltage-clamp protocol is shown in bottom panel. Middle right panel displays indicated part of current record at greater magnification to more optimally show the inhibitory effect of ryanodine on inward current during the voltage ramp. *Local $[Ca^{2+}]_i$ increase in the presence of ryanodine; #corresponding inward current inhibited in the presence of ryanodine.

(in 22 of 39 cells) a wavelike propagation along the long axis of the cell with velocity 50 to 100 $\mu\text{m/s}$, which is similar to what has been observed in cardiac myocytes and attributed to CICR.¹⁷ Thus, Ca^{2+} waves propagating locally and longitudinally beneath the sarcolemma during the DD serve to amplify the initial, localized pre-AP Ca^{2+} release. This pre-AP local Ca^{2+} release results in substantial refractoriness of the Ca^{2+} release process near the cell edge, given that the local Ca^{2+} increase in the same subsarcolemmal area evoked by Ca^{2+} influx during the ensuing AP upstroke is blunted (see second peak marked with an asterisk on the red curve in Figure 1B).

To further determine whether localized SR Ca^{2+} release via RYR is a mechanism of the pre-AP local $[Ca^{2+}]_i$ increase at the cell edge, as suggested but not proven by prior experiments,¹⁰ and to define its role in modulation of DD and SANC beating rate, also suggested but not proven by in prior studies,¹⁰ we determined the effects of ryanodine (a specific inhibitor of RYR) on the localized, pre-AP $[Ca^{2+}]_i$ transient and on SANC beating rate. In control, the spontaneous SANC beating rate was 176 ± 6 bpm ($n=27$). Ryanodine, in a dose-dependent manner, reduced the SANC beating rate and abolished beating (Figure 2A). This result is in accord with that of prior studies in subsidiary pacemaker cells from cat right atrium¹⁸ (1 $\mu\text{mol/L}$); in guinea pig SANCs¹⁹ (2 to 10 $\mu\text{mol/L}$); in cultured rabbit SANCs⁸ (10 $\mu\text{mol/L}$), in which ryanodine concentration reduced the beating rate by 63%, 30%, and 32%, respectively; and in toad pacemaker cells, in which ryanodine abolished spontaneous beating.³ Our results

further demonstrate that the reduction of SANC beating rate by ryanodine ($IC_{50}=2.6$ $\mu\text{mol/L}$) is accompanied by an abolition of the local, subsarcolemmal Ca^{2+} release during the DD preceding the AP upstroke (Figure 2B), indicating that the local Ca^{2+} increase is, in part at least, due to SR Ca^{2+} release via RYR. This indicates a pivotal role of the pre-AP Ca^{2+} release localized to the cell edge in spontaneous SANC firing, ie, in SANC automaticity.

If the localized, pre-AP local SR Ca^{2+} release were to activate an inward current, it would augment the slope of DD within the range of -60 and -30 mV, and it follows that inhibition of SR Ca^{2+} release should decrease this inward current. To test this hypothesis, we examined the effect of ryanodine on the pre-AP $[Ca^{2+}]_i$ transient localized to the cell edge and the simultaneously measured inward current under voltage clamp by using a voltage ramp to simulate the DD. As shown in Figure 2C, in the presence of ryanodine, the local $[Ca^{2+}]_i$ increase during the voltage ramp (asterisk in Figure 2C) was abolished, and inward current during the ramp was suppressed (see #, inset), confirming the idea¹⁰ that Ca^{2+} release from SR amplifies the DD in SANCs. Note that, whereas 3 $\mu\text{mol/L}$ ryanodine inhibited the inward current during the low-voltage ramp (by 1.59 ± 0.31 pA/pF at -40 mV, $n=4$), the peak $I_{Ca,L}$ (ie, the ionic current that underlies the AP upstroke) was unchanged. This demonstrates the crucial role of SR Ca^{2+} release via RYR in the augmentation of inward current during DD, and of its link to the spontaneous beating rate in SANCs.

It has been hypothesized,^{3,10} but not proven, that the NCX is a partner of the RYR in DD amplification, and thus a factor that modulates the beating rate of SANCs. To substantiate this hypothesis, we substituted lithium for sodium in the bath solution to block the NCX. Figure 3A shows that SANC beating is abolished just after superfusion with Li^+ -containing solution, which abolishes NCX and the generation of its inward current²⁰; with Li^+ washout the spontaneous beating resumes, demonstrating that NCX current is a prerequisite for spontaneous beating. However, it might be argued that such superfusion with Li^+ induces an increase in steady $[Ca^{2+}]_i$ during the DD, which in turn may affect SR loading, refractoriness of RYR, or currents involved in automaticity. Therefore, in additional experiments we used rapid superfusion ($t_{1/2}$, 200 to 300 ms) of a solution, in which Na^+ was completely substituted by Li^+ . As Figure 3B illustrates, the short-lasting, rapid superfusion with Li^+ solution blocks the subsequent SANC AP, leaving instead a DD with a slope of less than that of the previous beat in Na^+ containing superfusate. Moreover, the DD during the rapid superfusion without Na^+ is still accompanied by a local subsarcolemmal $[Ca^{2+}]_i$ transient having an amplitude of $\approx 70\%$ of that preceding the AP of the beat before Li^+ substitution for Na^+ . However, even this large Ca^{2+} release during DD in the presence of rapid Li^+ -induced NCX blockade is not adequate to promote sufficient DD to fire the anticipated subsequent AP. These experiments demonstrate that the NCX function is required for spontaneous SANC beating and therefore for cardiac pacemaker function.

To link the Li^+ substitution for Na^+ effect on DD to spontaneous AP firing in SANC beating to changes in inward

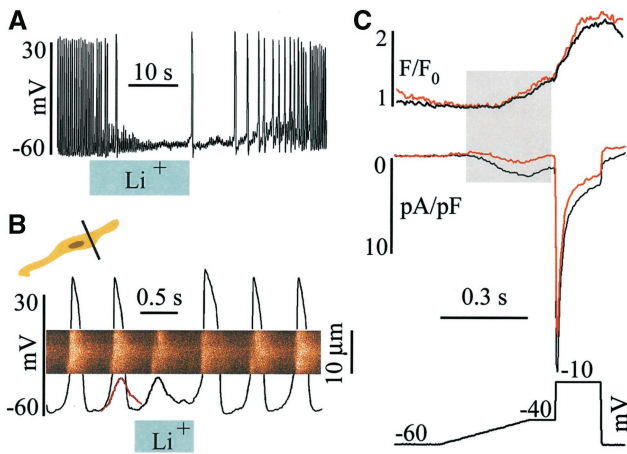


Figure 3. Inhibitory effect of Na^+ replacement by Li^+ on spontaneous beating in SANCs. **A**, AP recordings during onset and after washout of Na^+ -free, Li^+ -containing solution. Representative trace of 7 independent experiments is shown. **B**, Linescan image of Ca^{2+} release with superimposed AP records during rapid and brief superfusion with a solution in which Na^+ was replaced by Li^+ . Note that the maneuver blocked the subsequent AP firing. Scanned line was oriented perpendicular to long cell axis at half its depth (inset). Red curve superimposed on the last AP preceding spritz of Na^+ -free solution is a copy of the residual membrane potential oscillation observed during the Li^+ solution spritz. A representative recording of 3 independent experiments is shown. **C**, Normalized fluorescence (top), and membrane current (middle) during voltage clamp before (black) and 10 seconds after (red) superfusion with Na^+ -free, Li^+ -containing solution during voltage protocol (bottom). Highlighted area shows an inhibitory effect of Na^+ -free Li^+ spritz on inward current during the voltage ramp. A representative recording of 4 independent experiments is shown.

current during the DD, a voltage ramp was used to simulate DD. Figure 3C shows that substituting Li^+ for Na^+ in the superfusate while leaving Ca^{2+} release during DD unchanged ($P > 0.1$, $n = 3$) suppresses the inward current developed during the voltage ramp by 1.74 ± 0.35 pA/pF ($n = 4$), ie, by the same magnitude as the inhibition by ryanodine, suggesting that a major component of the inward current underlying the DD is, in fact, the NCX current. It is also important to note in Figure 3C that rapid modulation of SANC beating rate by Li^+ substitution for Na^+ occurs in the presence of an essentially unaltered $I_{\text{Ca,L}}$. Additional experiments (not shown) also demonstrated that rapid Li^+ superfusion does not affect I_f . Thus, we demonstrated directly that, in the presence of normal SR function, the AP firing in SANCs can be rapidly abolished by rapid replacement of superfusate Na^+ by Li^+ , ie, by rapid blockade of the NCX. Thus, RYR activation of NCX in SANCs is crucial to the occurrence of a spontaneous AP and thus to SANC pacemaker function.

In summary, the present novel observations, interpreted in the context of prior results,^{3,10} permit further definition of a recurrent chain of molecular events that underlies the heart pacemaker. The resultant perspective is that, first, after a short SANC AP plateau, outward K^+ currents²¹ drive the membrane potential to the minimum “diastolic” level that, in turn, activates inward I_f .^{22,23} Subsequently, the net current direction becomes inward, depolarizes the

membrane, and activates $I_{\text{Ca,T}}$ ^{10,24} and $I_{\text{Ca,L}}$ ^{25,13} resulting in Ca^{2+} influx sufficient to trigger a local Ca^{2+} release from the SR via RYR, as measured in the present study in SANCs and suggested in prior studies in atrial pacemaker cells.¹⁰ This local subsarcolemmal $[\text{Ca}^{2+}]_i$ transient, as demonstrated here, spreads locally in a wavelike manner to amplify via CICR the SR activation of NCX, which provides sufficient “booster inward current” to augment DD sufficiently to activate remaining dormant L-type channels to trigger an AP. As shown in the present study, inactivation of either RYR or NCX reduces or can abolish SANC automaticity. Thus, with optimal interactions of multiple diverse SANC sarcolemmal ion channels, the RYR and NCX permit spontaneous AP to occur and modulate the AP firing rate. The partnership of these two Ca^{2+} regulatory molecules in the context of the entire chain of diverse ion currents, as discovered in prior experiments,^{3,10,26,27} is an essential component both of the origin of the heartbeat and of its beating rate.

Acknowledgments

This work was supported by the NIH intramural research programs (grants to E.G.L.) and by grants from the National Research Council (to K.Y.B. and T.M.V.). We thank Drs M.D. Stern, H. Cheng, and I.R. Josephson for comments on the manuscript and Dr H.A. Spurgeon for help and technical support.

References

- Hagiwara N, Irisawa H, Kasanuki H, Hosoda S. Background current in sino-atrial node cells of the rabbit heart. *J Physiol.* 1992;448:53–72.
- Guo J, Ono K, Noma A. A sustained inward current activated at the diastolic potential range in rabbit sino-atrial node cells. *J Physiol.* 1995; 483:1–13.
- Ju YK, Allen DG. Intracellular calcium and Na-Ca exchange current in isolated toad pacemaker cells. *J Physiol.* 1998;508:153–166.
- Irisawa H, Brown HF, Giles W. Cardiac pacemaking in the sinoatrial node. *Physiol Rev.* 1993;73:197–227.
- DiFrancesco D. Pacemaker mechanisms in cardiac tissue. *Annu Rev Physiol.* 1993;55:455–472.
- Zhang H, Holden AV, Kodama I, Honjo H, Lei M, Varghese T, Boyett MR. Mathematical models of action potentials in the periphery and center of the rabbit sinoatrial node. *Am J Physiol.* 2000;279:397–421.
- Bassani RA, Bassani JW, Lipsius SL, Bers DM. Diastolic SR Ca efflux in atrial pacemaker cells and Ca-overloaded myocytes. *Am J Physiol.* 1997;273:H886–H892.
- Li J, Qu J, Nathan RD. Ionic basis of ryanodine’s negative chronotropic effect on pacemaker cells isolated from the sinoatrial node. *Am J Physiol.* 1997;273:H2481–H2489.
- Ju YK, Allen DG. The mechanisms of sarcoplasmic reticulum Ca^{2+} release in toad pacemaker cells. *J Physiol.* 2000;525:695–705.
- Huser J, Blatter LA, Lipsius SL. Intracellular Ca^{2+} release contributes to automaticity in cat atrial pacemaker cells. *J Physiol.* 2000;524:415–422.
- Fabiato A. Calcium-induced release of calcium from the cardiac sarcoplasmic reticulum. *Am J Physiol.* 1983;245:C1–C14.
- Sommer JR, Jennings RB. Ultrastructure of cardiac muscle. In: Fozzard HA, Haber E, Jennings RB, Katz AM, Morgan HE, eds. *The Heart and Cardiovascular System*. Vol 1. New York, NY: Raven Press; 1991:3–50.
- Vinogradova TM, Zhou YY, Bogdanov KY, Yang D, Kuschel M, Cheng H, Xiao RP. Sinoatrial node pacemaker activity requires Ca^{2+} /calmodulin-dependent protein kinase II activation. *Circ Res.* 2000;87: 760–767.
- Berlin JR. Spatiotemporal changes of Ca^{2+} during electrically evoked contractions in atrial and ventricular cells. *Am J Physiol.* 1995;269: H1165–H1170.
- Huser J, Lipsius SL, Blatter LA. Calcium gradients during excitation-contraction coupling in cat atrial myocytes. *J Physiol.* 1996;494: 641–651.

16. Cheng H, Lederer WJ, Cannell MB. Calcium sparks: elementary events underlying excitation-contraction coupling in heart muscle. *Science*. 1993;262:740–744.
17. Stern MD, Kort AA, Bhatnagar GM, Lakatta EG. Scattered-light intensity fluctuations in diastolic rat cardiac muscle caused by spontaneous Ca^{++} -dependent cellular mechanical oscillations. *J Gen Physiol*. 1983;82:119–153.
18. Rubenstein DS, Lipsius SL. Mechanisms of automaticity in subsidiary pacemakers from cat right atrium. *Circ Res*. 1989;64:648–657.
19. Rigg L, Terrar DA. Possible role of calcium release from the sarcoplasmic reticulum in pacemaking in guinea-pig sino-atrial node. *Exp Physiol*. 1996;81:877–880.
20. Blaustein MP, Lederer WJ. Sodium/calcium exchange: its physiological implications. *Physiol Rev*. 1999;79:763–854.
21. Ito H, Ono K. Role of rapidly activating delayed rectifier K^+ current in sinoatrial node pacemaker activity. *Am J Physiol*. 1995;269:H443–H452.
22. DiFrancesco D. The contribution of the “pacemaker” current (i_i) to generation of spontaneous activity in rabbit sino-atrial node myocytes. *J Physiol*. 1991;434:23–40.
23. Zaza A, Micheletti M, Brioschi A, Rocchetti M. Ionic currents during sustained pacemaker activity in rabbit sino-atrial myocytes. *J Physiol*. 1997;505:677–688.
24. Hagiwara N, Irisawa H, Kameyama M. Contribution of two types of calcium currents to the pacemaker potentials of rabbit sino-atrial node cells. *J Physiol*. 1998;395:233–253.
25. Verheijck EE, van Ginneken AC, Wilders R, Bouman LN. Contribution of L-type Ca^{2+} current to electrical activity in sinoatrial nodal myocytes of rabbits. *Am J Physiol*. 1999;276:H1064–H1077.
26. Terrar D, Rigg L. What determines the initiation of the heartbeat? *J Physiol*. 2000;524(pt 2):316.
27. Kass RS, Tsien RW. Fluctuations in membrane current driven by intracellular calcium in cardiac Purkinje fibers. *Biophys J*. 1982;38:259–269.